Development and Seismic Performance of Steel Dual-Core Self-Centering Braces

Chung-Che Chou
Professor, Dept. of Civil Engineering, National Taiwan University, Taiwan. cechou@ntu.edu.tw
Researcher, National Center for Research on Earthquake Engineering, Taiwan.

Ying-Chuan Chen
Graduate Student Researcher, Dept. of Civil Engineering, National Taiwan University, Taiwan.

SUMMARY
This work presents mechanics, tests, and finite element analyses of a proposed steel dual-core self-centering brace (SCB) with a flag-shaped hysteretic response under cyclic loads. The axial deformation capacity of the SCB is doubled by serial deformations of two sets of tensioning elements arranged in parallel. The mechanics and cyclic behavior of the brace are first explained; three 5350-mm long dual-core SCBs are tested and modeled to evaluate their cyclic performances. All SCBs exhibit excellent performance up to a target drift of 2% with a maximum tensioning element strain of 1%. All SCBs then successfully experience fifteen low-cycle fatigue tests at a drift of 1.5%. All SCBs are cyclically loaded again, and two SCBs achieve a drift of 2.5% with a maximum axial load of 1300 kN. Test results show that the application of dual cores in SCBs reduces significant strain demands on tensioning elements and enables self-centering responses to large deformation.

***Keywords**: Dual-core self-centering brace, Fiber-reinforced polymer tendon, Test, Finite element analysis*

1. INTRODUCTION

A buckling-restrained braced frame (BRBF) is considered as a good seismic-resisting braced system because a buckling-restrained brace (BRB) can yield in tension and compression without global buckling (Watanabe et al. 1988, Uang and Nakashima 2003, Usami et al. 2008, Tsai et al. 2008, Chou and Chen 2010a, Chou et al. 2011, Chou and Liu 2012). Despite numerous tests demonstrated satisfactory seismic performance of BRBs, the BRBF under earthquakes is prone to residual lateral deformation over the building height due to low post-yield stiffness and concentrated energy dissipation in braces (Uang and Kiggins 2003, Tremblay et al. 2008, Chou et al. 2012). Many researchers have demonstrated the effectiveness of applying post-tensioning (PT) technology to structural members to reduce residual lateral deformation of buildings or bridges under seismic loading (Priestley and MacRae 1996, Ricles et al. 2001, Christopoulos et al. 2002, Chou et al. 2006, Chou and Chen 2006). Static or dynamic tests on a post-tensioned self-centering (SC) moment frame that uses PT steel tendons to compress beams against columns further determine their satisfactory SC properties and energy dissipation (Pampanin et al. 2000, Lin et al. 2008, Chou and Chen 2010b, 2011a).

This work (Chou and Chen 2011b, 2012) presents the mechanics and seismic responses of a novel dual-core self-centering brace (SCB), which applies post-tensioning (PT) technology in the brace not in the beam to reduce the restraint from columns and slabs (Chou et al. 2008, Chou and Chen 2010c), as well as the residual drift of structures. A dual-core SCB consists of conventional steel bracing members, energy dissipative devices, and two tensioning element sets that are in a parallel arrangement. In comparison with a previous SCB (Christopoulos et al. 2008), the additional inner core and set of PT elements in the brace doubles the axial elongation capacity of the brace or halves the axial strain demands on PT elements of the brace. Therefore, the dual-core SCB makes it possible to adopt tendons with low elastic strain capacity without sacrificing deformation capability. Three 5350-mm long dual-core SCB, fabricated by a local steel fabricator, were tested at the National Center for Research on Earthquake Engineering (NCREE), Taiwan, with those results presented in this paper. Test parameters were tendon types and tendon diameters. Two dual-core SCBs used E-glass fiber reinforced polymer (FRP) composites as PT tendons and one specimen used T-700 carbon FRP

composites as PT tendons. All dual-core SCB specimens were subjected to two cyclic loading tests with increasing amplitudes and a 15-cycle fatigue loading test with fixed amplitude (1.5% drift). All specimens performed well up to a drift of 2% and also survived during additional 15-cycle fatigue loading test with fixed amplitude of 1.5% drift. Moreover, two specimens under additional cyclic loading performed well up to an interstory drift of 2.5% without structural damage and provided stable energy dissipation capacity with SC properties. The maximum strain in the tensioning element was 1.3%, and the maximum axial load in the brace was 1300 kN. One specimen under additional cyclic loading failed towards 2.5% drift because the tendon strain exceeded the tensile strain limit of E-glass FRP composites. Finally, finite element analysis is conducted on the specimens to perform a correlation study and then a parametric study to evaluate the effects of tensioning element types, initial PT force, and friction force on the cyclic performance of the dual-core SCB.

2. MECHANICS OF A DUAL-CORE SCB

2.1 Proposed Dual-core SCB

Figure 1 shows the proposed dual-core SCB, which consists of three steel bracing members, two PT element sets, energy dissipation devices, and end plates. Three steel bracing members are designated as the first core, second core, and outer box; all members have the same length. Two sets of tendons in the second core and outer box tube are anchored with nuts to the outer and inner end plates. Neither the bracing members nor the end plates are welded together. An energy dissipative device, which is located at the one end of the brace, is activated by the relative motion induced between the first core and outer box. All bracing members, end plates, and tendons in the dual-core SCB are arranged so that a relative motion induced between these bracing members causes serial elongation of the inner and outer tendons to achieve the desired brace elongation or shortening, which is always two times that of the tendon elongation. The brace self-centers if the initial PT force provided by the tendons exceeds the force required to activate the friction device.

2.2 Kinematics and Mechanics

Figure 2 presents the kinematics and hysteretic response of the dual-core SCB. Once the activation load, F_{dt}, of a dual-core SCB is exceeded, the inner end plate moves in opposite directions with respect to the outer end plate, resulting in a brace deformation twice that of the tendon elongation δ (Figure 2(a)). The activation load, F_{dt}, is expressed as

$$F_{dt} = \frac{nT_{in}}{2} + F_f \tag{1}$$

where T_{in} is the initial PT force in one tendon, F_f is the frictional force of the energy dissipative device, and n is the total number of tendons. Axial stiffness of the dual-core SCB changes from the axial stiffness of these bracing members to the postelastic stiffness, as determined by the axial stiffness of tendons and second core:

$$K_{pt} = \frac{1}{\frac{1}{\frac{n}{2}K_t} + \frac{1}{\frac{n}{2}K_t} + \frac{1}{K_{2c}}} \tag{2}$$

where K_{2c} is the axial stiffness of the second core and K_t is the axial stiffness of one tendon. The elongation in each tendon set δ causes the axial deformation of 2δ in the dual-core SCB. The brace returns to its original position when the load is removed (Figure 2(b)). The behavior of the brace under compression is similar to that under tension.

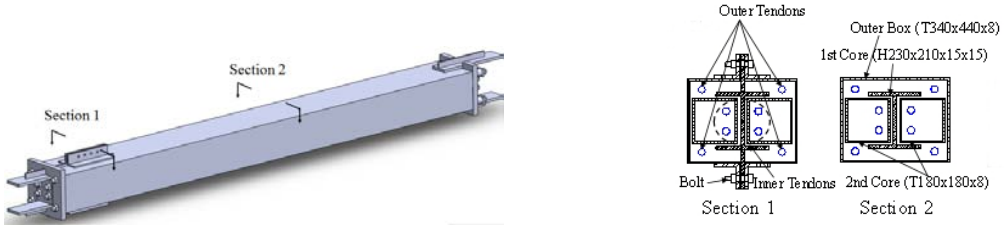

(a) Overall View (b) Section View

Figure 1. A proposed dual-core SCB

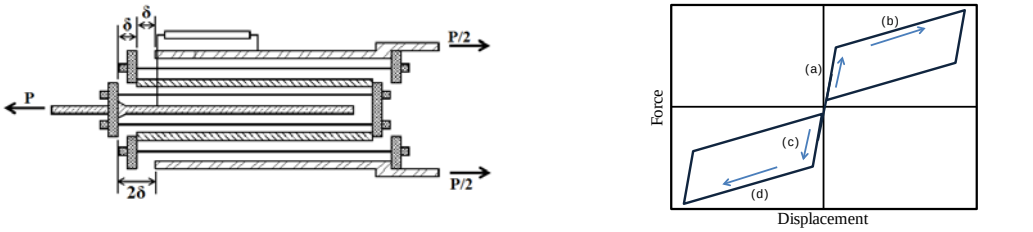

(a) Brace Kinematics (b) Force *versus* Displacement Relationship

Figure 2. Kinematics and hysteretic response of a proposed dual-core SCB

3. TESTS OF DUAL-CORE SCBs

3.1 Specimens

The test program consisted of cyclic tests of three dual-core SCB specimens. Each dual-core SCB had a first core of H230×210×15×15 mm, two second cores of T180×180×8 mm, and an outer box tube of T340×440×8 mm. All steel bracing members were identical in the three specimens. Specimens 1 and 2 had eight E-glass FRP tendons, and Specimen 3 had eight T-700 carbon FRP tendons (Table 1). The initial PT forces in the braces were set to 260 kN. The friction devices placed on one end of the braces were set to produce friction forces of 250 kN. The design force was 1000-1225 kN at the target drift of 2% in accordance with the FRP tendon strains of 1.07, 0.93, and 1.06% in the specimens, which were much lower than those in SCBs with only a single-core bracing member. All specimens were fabricated by a local steel fabricator and pot-tensioned at the National Center for Research on Earthquake Engineering (NCREE). The specimen was positioned in the test setup (Figure 3), which included one steel box column pin-supported to the laboratory floor and attached to two 1000-kN hydraulic actuators. The dual-core SCB specimen was positioned at an incline of θ=40° with both ends welded to dual gusset plates, which were designed to remain elastic at the ultimate strength level (Chou et al. 2011, 2012).

Table 1. Design and test values of dual-core SCBs

Specimen	Tendon Type	Tendon Diameter (mm)	Initial PT Force (kN)	2% Drift				
				Axial Force		Brace Strain (%)	Tendon Strain (%)	
				Tension (kN)	Compression (kN)		Double Core	Single Core
1	E-Glass Fibers	22.2	260 (260)	1025 (1060)	1000 (1133)	1.2 (1.16)	1.07 (1.02)	1.84
2	E-Glass Fibers	28.7	260 (290)	1225 (1415)	1180 (1359)	1.2 (1.09)	0.93 (0.86)	1.71
3	T-700 Carbon Fibers	12.7	260 (285)	1010 (1035)	990 (1193)	1.2 (1.2)	1.06 (1.07)	1.83

Table 2. Material properties of tensioning elements

Tendon Type	Diameter (mm)	Data Source	Elastic Modulus (GPa)	Ultimate Stress (MPa)	Ultimate Strain (%)
E-Glass Fiber	28.7	Manufacture	41	517	1.3
		Test	43	442	1.04
	22.2	Manufacture	41	586	1.4
		Test	45	657	1.47
T-700 Carbon Fiber	12.7	Manufacture	124	1724	1.5
		Test	141	1643	1.17

3.2 Four Loading Phases

The dual-core SCB specimens were subjected to four loading phases. The specimen was first tested to a drift of 0.5% in Phase 1 before stressing bolts in the friction device to evaluate initial PT force. In the following loading phases, eight F10T 20-mm-diameter bolts were used to stress the friction device. Each specimen was then subjected to the standard loading protocol specified in Section T6 of the AISC seismic provisions (2005) for evaluating the BRB performance. The loading protocol consisted of two cycles per column drift of 0.36, 0.5, 1, 1.5 and 2% (Phase 2). All specimens were subjected to an additional fifteen low-cycle fatigue loading at a column drift of 1.5% (Phase 3). The objective of the test was to evaluate the durability of the friction device and tendon-coupler anchorage. Finally, all specimens were reloaded under the standard loading protocol beyond the target drift of 2% until failure (Phase 4).

3.3 Test Results

3.3.1 Phase 1 and 2 Tests

Phase 1 test revealed a bilinear elastic response of the dual-core SCB; the change of stiffness occurred at a load equal to the initial PT force shown in the parenthesis in Table 1. Figure 4 shows the actuator force *versus* lateral displacement responses of specimens in Phase 2 test, and Figure 5 shows the corresponding axial force *versus* axial displacement responses of all braces. Axial deformation is measured from displacement transducers positioned on the ends of the dual-core SCB. The dual-core SCB developed stable energy dissipation and self-centering property up to an interstory drift of 2%. No damage in PT elements or steel bracing members was found in Specimens 1 and 2 throughout the test. Since Specimens 1 and 2 used eight 22-mm diameter and 28-mm diameter E-glass FRP tendons, respectively, the maximum axial force and post-elastic stiffness in Specimen 1 were smaller than those in Specimen 2 (Figure 5). Specimen 3 used eight 13-mm diameter T-700 carbon FRP tendons, and one FRP tendon-coupler anchorage fell off towards 2% drift, slightly decreasing the ultimate load and increasing the residual deformation compared to previous loading cycles (Figure 4(c) and Figure 5(c)). The activation load and initial elastic stiffness from the mechanics can reasonably match the hysteretic response. Since the friction force increases with cyclic displacements, which differs from the bilinear rigid-plastic response assumed in the typical friction mechanism, the model underestimates the axial force in the large axial displacement (Figure 5). This behavior can be overcome by replacing a friction device with a stable energy dissipating device.

3.3.2 Phase 3 and 4 Tests

Figure 6 shows the axial force-displacement responses of Specimens 1-3 under fifteen low-cycle fatigue loading at 1.5% drift (Phase 3). Noise induced by friction devices was significantly lower in Phase 3 test than in Phase 2 test. All specimens showed stable and re-centering properties throughout the test; no damage in tensioning elements or bracing members was observed after completing the test. Although one tensioning element of Specimen 3 failed in Phase 2 test, other tensioning elements maintained their elongation capacities without failure. The large residual deformation observed in Specimen 3 resulted from the friction force exceeding the initial PT force after loss of one tendon.

After a complete loading protocol in Phase 3 test, all specimens were reloaded with AISC loading protocol to a drift of 2.5%. When Specimen 1 was loaded in 2.5% drift cycles, the tendon strain was 1.23%, which was lower than its 1.47% capacity (Table 2). Therefore, no tensioning elements were damaged during the test (Figure 7(a) and 8(a)), and the maximum axial force in the brace was 1300 kN.

Specimen 2 survived the first cycle of compression test to a drift of -2.5%, but four outer tendons fractured when drift approached 2.5%, which led to loss of axial capacity near axial load of 1500 kN (Figure 7(b)). Specimen 3 competed two 2.5% drift cycles without tendon failure, and the brace was then loaded to a drift of 3%. The suddenly increased force (Figure 7(c)) resulted from the bearing between the bolts and slot holes in the friction device since the slots were designed to accommodate a brace elongation to 2.5% drift. Two inner tendons fractured at a strain of 1.27% (Figure 8(b)), which exceeded the strain limit of 1.17% for T-700 carbon fibers (Table 2).

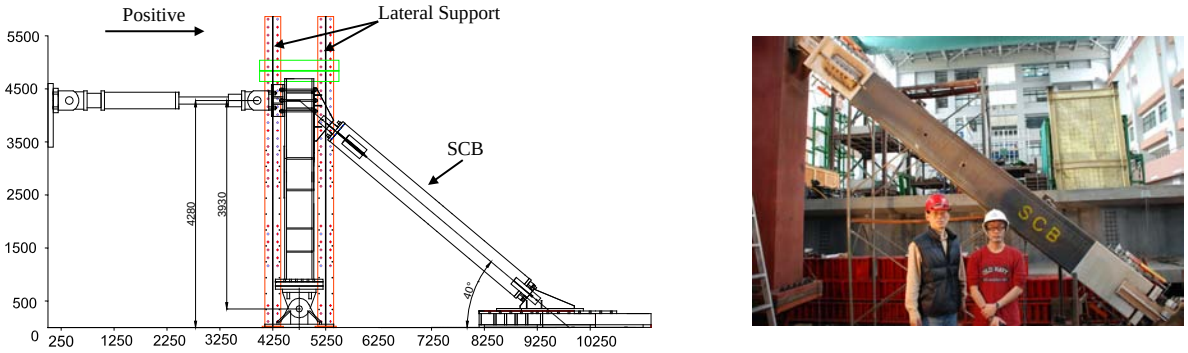

(a) Test Setup (unit: mm) (b) 2.5% drift

Figure 3. Test setup and overall deformation of the dual-core SCB

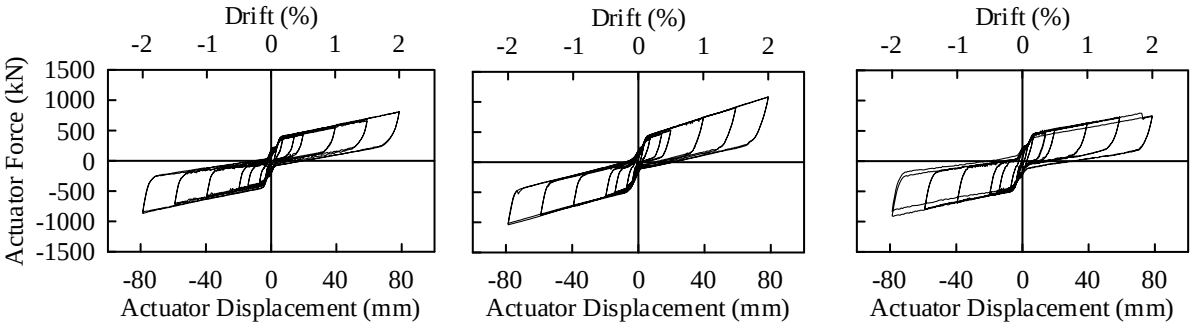

(a) Specimen 1 (b) Specimen 2 (c) Specimen 3

Figure 4. Actuator force versus displacement relationship of dual-core SCBs (Phase 2)

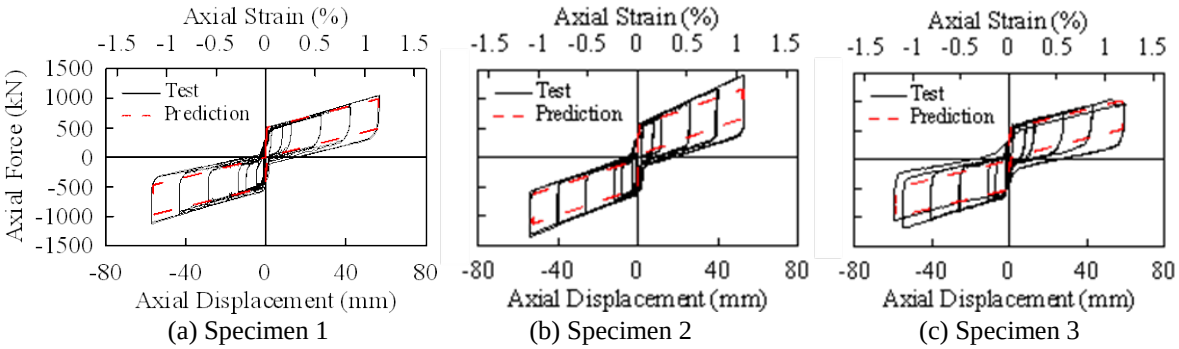

(a) Specimen 1 (b) Specimen 2 (c) Specimen 3

Figure 5. Axial force versus axial displacement relationship of dual-core SCBs (Phase 2)

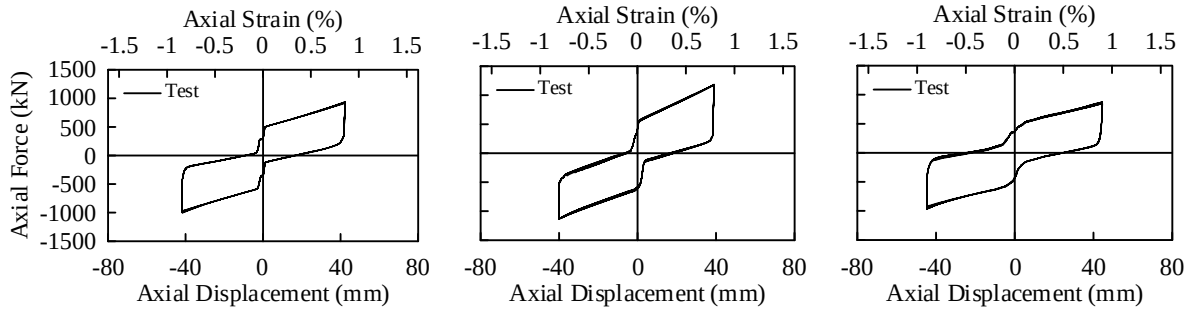

Figure 6. Axial force versus axial displacement relationship of braces under 15-cycle fatigue loading (Phase 3)

4. FINITE ELEMENT ANALYSES

4.1 Specimen Model

To further study the self-centering behavior of dual-core SCBs, an analytical study using the finite element computer program ABAQUS (2009) was conducted on the specimens. Specimens described in the previous section were analyzed for a correlation study. Material nonlinearity with the von Mises yielding criterion was considered in the steel bracing members. A tendon made of FRP composites was modeled with only linearly elastic properties. Figure 9(a) shows a three-dimensional model of the specimen after assembly. Axial displacement obtained from the test was used as a controlling parameter in the finite element analysis. When the axial force in the brace exceeds the activation load, the inner and outer end plates begin to move with respect to the bracing members as observed in the test. Figure 9(b) shows that the brace in tension produces a relative displacement between the left inner end plate and the outer box, Δ_2, twice that between the left outer end plate and the outer box, Δ_1. Opening behavior observed on the right end in compression is similar to that observed on the left end in tension. Figure 9(c) and (d) show that the specimen in the first cyclic test performs as the finite element analysis; the variation in tendon force is symmetrical under both tension and compression.

4.2 Parametric Study

This work also evaluates the cyclic performances of dual-core SCBs with different structural characteristics by modeling 16 dual-core SCBs through use of the computer program ABAQUS (2009). All models have the same steel member size as that of the specimen; the parameters include material type of tendons, diameter of tendons, initial PT force, and friction force (Table 3). The first two characters (SS, GF, or CF) of the model ID stand for the material property of tendons (Steel Strands, Glass Fiber, or Carbon Fiber). The third character (D) with the following number of the model ID identifies the diameter of tendons in the unit of mm. The character of LPT or SPT represents large or small initial PT forces, respectively. Since steel tendons have a smaller elastic strain limit than that of FRP tendons, the initial PT force in the steel tendons is smaller than that in the FRP tendons to maintain the self-centering properties. The last two characters LF or SF represent large or small friction forces, respectively. The self-centering property of the dual-core SCB can be maintained when the friction force is smaller than the initial PT force. For some models with a friction force larger than the initial PT force, the cyclic performances of dual-core SCBs with residual drifts can be evaluated. Figure 10 shows the effects of friction force and initial PT force on the hysteretic responses of dual-core SCBs. Figure 10(a) shows that a large friction force causes both large energy dissipation and residual displacement if the friction force exceeds the initial PT force. When the initial PT force is increased, the residual displacement becomes zero, maintaining full re-centering property (Figure 10(b)).

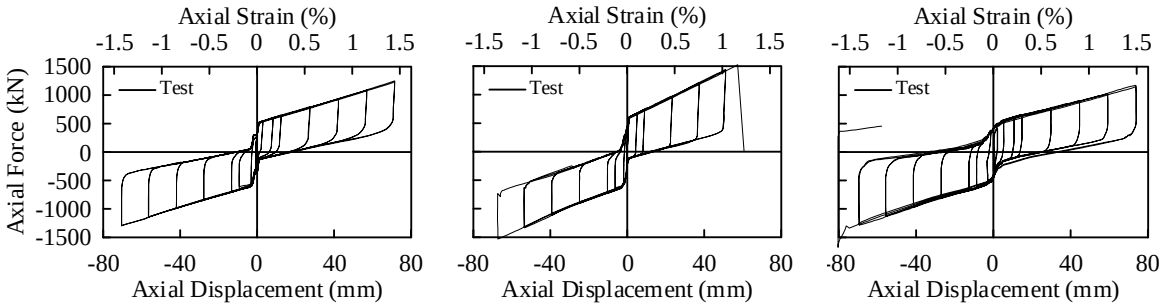

(a) Specimen 1 (b) Specimen 2 (c) Specimen 3

Figure 7. Axial force versus axial displacement of dual-core SCBs under cyclic loading (Phase 4)

(a) Specimen 1 (2.5% drift) (b) Specimen 3 (towards 3% drift)

Figure 8. Specimen performance (Phase 4)

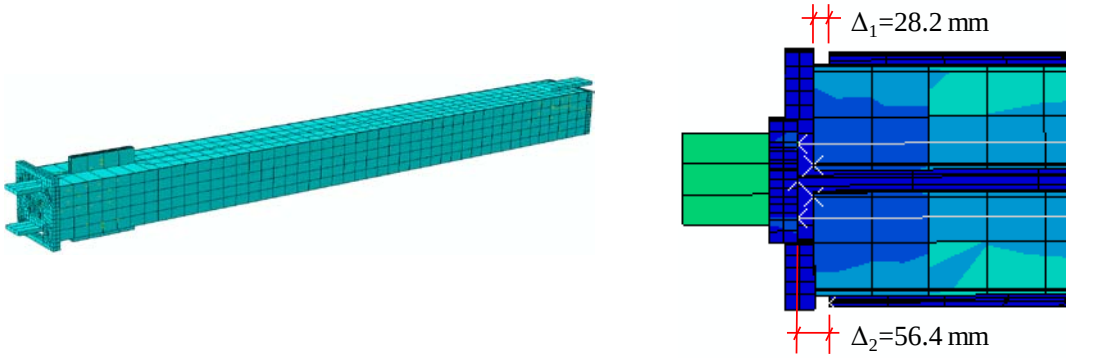

(a) A Dual-Core SCB Model (b) A Dual-Core SCB Model in Tension

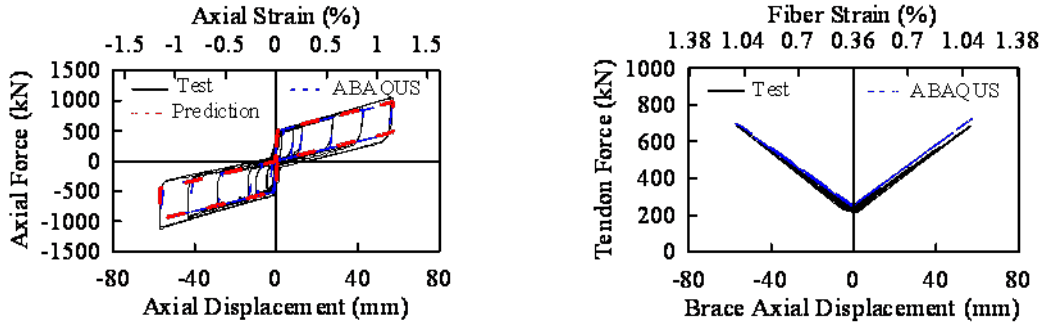

(c) Hysteresis Response (d) Inner Tendon Force

Figure 9. Comparison between the cyclic test and finite element analysis (Specimen 1)

Table 3. Finite element models

Model		Tendon		Initial PT Force (kN)	Friction Force (kN)
No.	ID	Material	Diameter (mm)		
1	SSD16SPTSF	Steel Strand	15.2	130	128
2	SSD16SPTLF				256
3	SSD16LPTSF			260	128
4	SSD16LPTLF				256
5	GFD22SPTSF	E-Glass Fiber	22.2	160	158
6	GFD22SPTLF				316
7	GFD22LPTSF			320	158
8	GFD22LPTLF				316
9	GFD29SPTSF		28.7	160	158
10	GFD29SPTLF				316
11	GFD29LPTSF			320	158
12	GFD29LPTLF				316
13	CFD13SPTSF	T700-Carbon Fiber	12.7	160	158
14	CFD13SPTLF				316
15	CFD13LPTSF			320	158
16	CFD13LPTLF				316

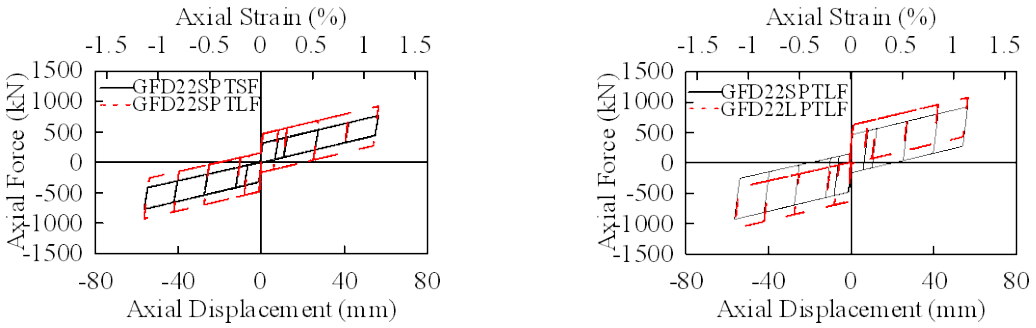

(a) Friction Force Effects (b) Initial PT force Effects

Figure 10. Effects of friction force and initial PT force on dual-core SCB responses

5. CONCLUSIONS

This work presents mechanics, test and finite element analysis results of a new dual-core self-centering brace (SCB) with three steel bracing members for compression, two sets of tensioning elements for self-centering, and friction devices for energy dissipation. Validation tests were performed on three 5350-mm long dual-core SCBs with tensioning elements fabricated from E-glass or T-700 carbon fiber reinforced polymer composites. Four loading phase tests were performed to evaluate the cyclic response, elongation capacity, and durability of the dual-core SCBs.

Tests and finite element analyses confirmed that the dual-core SCB performs as predicted by the mechanics and its elongation capacity is doubled mainly by serial deformations of two tensioning element sets. The proposed dual-core SCB reduces the need for tendons with high elongation capacity, so widely varying tendons can be used as re-centering elements. Good energy dissipation and good re-centering properties of the dual-core SCBs are ensured within the design target drift of 2%; repeatable flag-shaped responses under 15 low-cycle fatigue loading are also achieved at 1.5% drift. During the fourth cyclic test, two dual-core SCBs achieve a drift of 2.5% with a maximum axial load of 1300 kN, and one dual-core SCB fails near the axial load of 1500 kN because the tensile strains in FRP tendons exceed the elongation capacity of tendons. The finite element model can predict the flag-shaped response of the dual-core SCB under the cyclic test. A large friction force produces large energy dissipation and causes residual deformation if it exceeds the initial PT force. When the initial PT force is increased, the residual displacement becomes zero, maintaining full re-centering property.

ACKNOWLEDGMENTS

The authors would like to thank the National Science Council, Taiwan for financially supporting this research under Contract No. *NSC 99-2625-M-002-016*. The authors would also like to thank Prof. K. C. Tsai in providing valuable advices in the program.

REFERENCES

AISC. 2005. *Seismic provisions for structural steel buildings*, American Institute of Steel Construction, Chicago.

Chou C-C, Chen Y-C. (2006). Cyclic tests of post-tensioned precast CFT segmental bridge columns with unbonded strands. *Earthquake Engineering and Structural Dynamics*, 35, pp. 159-175.

Chou C-C, Chen J-H, Chen Y-C, and Tsai K-C. (2006). Evaluating performance of post-tensioned steel connections with strands and reduced flange plates. *Earthquake Engineering and Structural Dynamics***,** 35(9): 1167-1185.

Chou C-C, Weng C-Y, Chen J-H. (2008). Seismic design and behavior of post-tensioned connections including effects of a composite slab. *Engineering Structures*, 30, pp. 3014-3023.

Chou C-C, Jao C-K. (2010). Seismic rehabilitation of welded steel beam-to-box column connections utilizing internal flange stiffeners. *Earthquake Spectra*, 26(4), 927-950.

Chou C-C, Chen S-Y. (2010a). Subassemblage tests and finite element analyses of sandwiched buckling-restrained braces. *Engineering Structures*, 32, 2108-2121.

Chou C-C, Chen J-H. (2010b). Tests and analyses of a full-scale post-tensioned RCS frame subassembly. *J. Constructional Steel Research*, 66(11), 1354-1365.

Chou C-C, Chen J-H. (2010c). Column restraint in post-tensioned self-centering moment frames. *Earthquake Engineering and Structural Dynamics*, 39(7), 751-774.

Chou C-C, Chen J-H. (2011a). Seismic design and shake table tests of a steel post-tensioned self-centering moment frame with a slab accommodating frame expansion. *Earthquake Engineering and Structural Dynamics*, 40 (11), 1241-1261.

Chou C-C, Chen Y-C. (2011b). Seismic performance of a post-tensioned self-centering energy dissipative brace. *Report No. NSC 99-2625-M-002-016*, National Science Council, Taiwan. (in Chinese)

Chou C-C, Liu J-H, Pham D-H. (2011). Steel buckling-restrained braced frames with single and dual corner gusset connections: seismic tests and analyses. *Earthquake Engineering and Structural Dynamics* (available on line 2011/10).

Chou C-C, Liu J-H. (2012). Frame and brace action forces on steel corner gusset plate connections in buckling-restrained braced frames. EQS-112410EQS197M.3d, *Earthquake Spectra* (published in 2012/5).

Chou C-C, Liou G-S, Yu J-C. (2012). Compressive behavior of dual-gusset-plate connections for buckling-restrained braced frames. doi:10.1016/j.jcsr.2012.03.003, *J. Constructional Steel Research* (accepted, published in 2012/7).

Chou C-C, Chen Y-C. (2012). Development of steel dual-core self-centering braces with E-glass FRP composite tendons: cyclic tests and finite element analyses. *The International Workshop on Advances in Seismic Experiments and Computations*, Nagoya, Japan.

Chou C-C, Chen Y-C, Pham D-H, Truong V-M. (2012). Experimental and analytical validation of steel dual-core self-centering braces for seismic-resisting structures. *9th International Conference on Urban Earthquake Engineering/4th Asia Conference on Earthquake Engineering*, Tokyo, Japan.

Christopoulos C, Filiatrault A, Uang CM, Folz B. (2002). Posttensioned energy dissipating connections for moment-resisting steel frames. *J. Struct. Engrg.*, ASCE; 128(9): 1111-1120.

Christopoulos C, Tremblay R. Kim H-J, Lacerte M. (2008). Self-centering energy dissipative bracing system for the seismic resistance of structures: development and validation. *J. Struct. Engrg.*, ASCE, 134(1), 96-107.

HKS, 2009. *ABAQUS User's Manual Version 6.9*, Hibbitt, Karlsson & Sorensen, Pawtucket, RI.

Lin Y-C, Ricles JM, and Sause R. (2008). Earthquake simulations on a self-centering steel moment resisting frame with web friction devices, *14th World Conference on Earthquake Engineering*, Beijing, China.

Priestley MJN and MacRae GA. (1996). Seismic tests of precast beam-to-column joint subassemblages with unbonded tendons. *PCI Journal*, January-February, 64-80.

Pampanin S, Priestley MJN, Sritharan S. (2000). PRESSS Phase 3: the five-story precast test building-frame direction response. Report No. SSRP 2000/08. University of California San Diego, La Jolla, CA.

Ricles JM, Sause R, Garlock MM, and Zhao C. (2001). Posttensioned seismic-resistant connections for steel frames. *J. Structural Engineering*, ASCE, 127(2), 113-121.

Tremblay R, Lacerte M, Christopoulos C. (2008). Seismic Response of Multistory Buildings with Self-Centering Energy Dissipative Steel Braces *J. Structural Engineering*, ASCE, 134, 108-120.

Tsai K-C, Hsiao B-C, Wang K-J, Weng Y-T, Lin M-L, Lin K-C, Chen C-H, Lai J-W, Lin S-L. (2008). Pseudo-dynamic tests of a full scale CFT/BRB frame-Part I: Specimen design, experiment and analysis. *Earthquake Engineering and Structural Dynamics*, 37: 1081-1098.

Uang C-M, Nakashima M. (2003). Steel buckling-restrained braced frames. In Earthquake Engineering from Engineering Seismology to Performance-based Engineering (Chapter 16). CRC Press LLC: Boca Raton, FL.

Uang C-M, Kiggins S. (2003). Reducing residual drift of buckling-restrained braced frames. *Int. Workshop on Steel and Concrete Composite Construction*, *Report No. NCREE-03-026*, National Taiwan University, Taiwan.

Usami T, Ge HB, Kasai A. (2008). Overall buckling prevention condition of buckling-restrained braces as a structural control damper. *14th World Conference on Earthquake Engineering*, Beijing, China.

Watanabe A, Hitomi Y, Yaeki E, Wada A, and Fujimoto M. (1988). Properties of braces encased in buckling-restraining concrete and steel tube. *9th World Conference on Earthquake Engineering*. Tokyo-Kyoto, Japan, 719-724.